SINGLE MOLECULE FORCE EXTENSION MEASUREMENT ON SEMI-FLEXIBLE BIOPOLYMERS USING MAGNETIC TWEEZERS

BY

SUN JU KIM

THESIS

Submitted in partial fulfillment of the requirements
for the degree of Master of Science in Chemical Engineering
in the Graduate College of the
University of Illinois at Urbana-Champaign, 2010

Urbana, Illinois

Adviser:

Professor Charles Schroeder

Abstract

Polymers are pervasive in modern society and are commonly encountered in a wide-range of industrial processes. Polymer chains exhibit complex dynamical phenomena in solutions undergoing convective transport, and a proper understanding of chain dynamics is key to optimizing process conditions. The molecular structure of a polymer chain ultimately determines the macroscopic mechanical response and overall physical properties of polymer solutions and melts. Therefore, the study of polymer chain dynamics is essential to understanding the relationship between polymer chain structure and function. In this thesis, the elasticity of semi-flexible polymers is characterized using double stranded lambda-phage DNA. Single DNA molecules are studied using magnetic tweezers and an inverted fluorescence microscope. Magnetic forces in the piconewton range are applied to individual DNA molecules, and the relative chain extension due to applied force is directly measured and shown to be between 15% and 75% of the polymer contour length (16.3 μm for lambda-phage DNA). The results obtained from this experiment compare favorably to the analytical formula for DNA elasticity derived by Marko and Siggia and previous experimental data obtained using an optical tweezers assay. In addition, a magnetic tweezers set up has been designed, constructed and validated, and this single molecule assay can be further used to study novel polymeric systems, such as chemically-modified single stranded DNA, a flexible polymer. Overall, the research presented in this thesis provides the groundwork for novel investigation of novel polymeric systems at the single molecule level.

TABLE OF CONTENTS

Chapter 1

INTRODUCTION

1.1 Study of Polymers

The ability to study phenomena at nano and even picometer scales has enabled the study of single molecules and the design and fabrication of nanofluidic devices. Such changes in scales have allowed researchers to better build a fundamental understanding of various materials. Of importance is the study of polymer dynamics, a material that is of utmost prevalence in our lives.

Recent development in single molecule studies has led researchers to monitor individual polymer chains, real time. Such direct observation of each polymer chain, and therefore knowledge of their true backbone dynamics, was not possible with past bulk measurements, such as viscosmetry, light scattering experiments and velocity sedimentation [1, 2]. Results from these techniques were based on an ensemble average of multiple polymer chains and therefore do not account for the poly-dispersity of a given sample. This therefore obscures real-time dynamical behavior of single chains and does not allow for characterization of molecular subpopulation. With the new single molecule technique using fluorescent microscopy and microfluidic devices, important polymer properties, such as stretching dynamics in various flow types [2, 3], the relaxation behavior [4], and conformational hysteresis in extensional flow [5], has been directly visualized.

Using single molecule techniques, the responses of polymers to various types and magnitude of forces can be understood with more precision [6-8]. Such knowledge is crucial in order to understand the polymers' mechanical and elastic properties [9-13], which are directly related to their various applications. The new single molecule technique overcomes inaccuracy in results that arises in past bulk measurements from preaveraging variables such as hydrodynamic interaction tensor [2]. Especially of growing interest are the stretching dynamics due to forces of biopolymers, which are biodegradable. They can be used in areas such as drug delivery, tissue engineering, and medical device fabrication in place of synthetic polymers with higher compatibility, performance and lower cost.

The relationship between force and extension of biopolymers, and therefore its elastic properties, are necessary in understanding their complicated properties and activities in biological systems [14, 15]. The elastic properties of a biopolymer allow one to understand its molecular structure, and how dependent the polymer's structure is on the various forces inherent in the polymer and the external forces that are exerted on the biopolymer. Moreover, as the functions of many biopolymers are highly related to their structure, obtaining the knowledge of their response to forces can give us an idea of their complicated roles in various systems. Specific biological interactions such as induced-fit molecular recognition between proteins and DNA, or folding of DNA into chromosomes can be understood by studying the force extension relationship [13, 16].

More fundamentally, experimental results obtained from these measurements can lead to information as to how different theoretical models, such as the wormlike chain (WLC)

and freely joint chain (FJC) models can be used to classify polymer systems based on their stretching dynamics [8, 10, 11].

1.2 Force Extension Measurements

There are number of different experimental methods through which force extension measurements can be made on single molecular level. The most basic and widely used methods that are used include atomic force microscope (AFM), optical tweezers, and magnetic tweezers.

AFM is a sensitive single molecule tool that can be used to measure force on single molecule chains directly [17]. AFM is a scanning probe microscopy that allows manipulation of a given material at nanoscales, using which 3-dimensional positions of a sample surface or the force-extension measurements can be made [18]. Both measurements can be made from the tip sharpness and the cantilever spring constant, values that can be estimated based on the motion of the movement of the tip above the sample.

Different types of methods exist to measure the elasticity of polymers using AFM. The idea that has been used by many research groups is that the bent cantilever to which the probe is connected applies stress onto the polymer chain of interest and the force from interaction between the tip and the polymer chain can be measured with respect to distance [17]. In experiments using the AFM, the polymer chains are placed on a substrate (for example mica substrates), with high density coverage. The tip of the AFM probe is pushed into and pulled back out of the DNA molecules repeatedly at different points, so

that force at different lengths can be measured. AFM image also shows x-y or 3D positions of the polymer chains depending on the type of the probe that is used.

Optical tweezers are also a widely used single molecule tool to make force extension measurements [19-21]. This technique is commonly known as optical trap. A laser beam passes through a series of lenses, and beam splitters, depending on the experimental set up. The final objective lens focuses the laser beam that passes through, and the focused beam consists of strong electric field gradient. As this focused beam comes in contact with the particle of interest the beam is refracted and results in light scattering and gradient forces, and these forces causes the particle to be trapped in the center. Therefore, particles such as microscopic dielectric beads that are tethered to one end of the polymer chain can be trapped. The displacement of the bead relative to the center of the trap is proportional to the force that is exerted on the bead. Measurement of the displacement of the bead interferometrically relative to the trap that is formed using the laser leads to knowledge of the force extension on a given polymer chain.

Magnetic tweezers represent another method to make force extension measurements, and are used by many groups to determine the force extension relationship of polymer chains [6, 9, 22-25]. Using this technique, a polymer chain is functionalized so that it has a functional group that can form a bond with a magnetic bead on one end. The magnets are mounted above the beads. The other end of the polymer chain is tethered to a surface, for example a coverslip, using conjugation between substances that have high affinity for one another, such as biotin and streptavidin, or DIG and anti-DIG. The magnets

exert a magnetic force on the beads and extend the polymer chains to various lengths depending on the distance of the magnet from the magnetic bead, which changes the magnitude of the magnetic force. Observations of the Brownian motion of the beads and their relative change in distance from the surface in the z-direction, provides the magnitude of the force exerted on the magnetic beads with respect to extension of the polymer chain.

Magnetic tweezers generally exert smaller scale forces compared to AFM and optical tweezers. AFM can generally exert force on the scale of 20pN up to 1nN, and optical tweezers can exert force between 5pN and 100pN. The sample polymers for which force extension measurements have been made in this experiment set up required forces ranging between 0.1pN and at maximum 50pN. Use of magnetic tweezers is a very suitable method to measure force in this range, we therefore used magnetic tweezers for this experiment.

1.3 Theoretical Background

In this experimental set up, the sample polymer to be used is tethered to a surface on one end, with the other end free to move in the solution within the flow cell (figure 1.1).

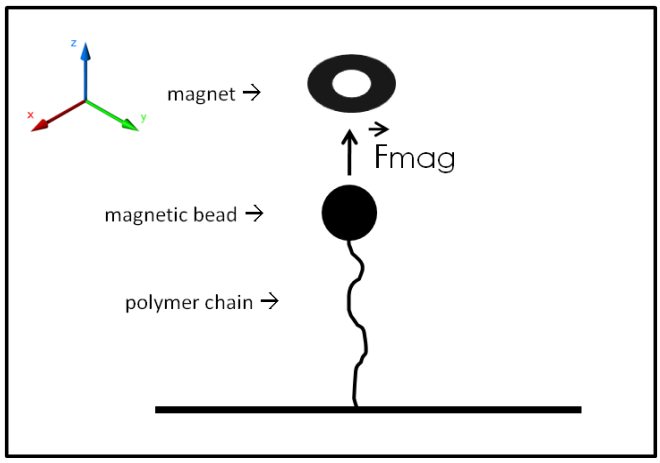

Figure 1.1: Polymer chain tethered to surface on one end, with magnetic force acting on the other end that has magnetic bead tether

Rare earth magnets (NdFeB) exert forces on the magnetic bead tethered to the polymer, and the magnitude of the force depends on the proximity and the net strength of the stacked magnets. In the low force regime, this configuration is analogous to an ideal Hookean bead-spring model, where the spring is bound to a surface on one end and free to stretch on the other. The bead exhibits Brownian motion but as it is tethered to the polymer on one end, its motion that undergoes thermal fluctuation is dependent on the elastic properties of the sample polymer chain and the magnitude of the applied magnetic force.

Calculation of spring constants and the energy balance of this system allow us to derive the relationship between the applied magnetic force and the corresponding extension of the sample polymer.

In the direction parallel to the sample polymer chain, the displacement of the chain due to Brownian fluctuation is very small and therefore, the force in this direction can be expressed and expanded in a Taylor series (Figure 1.2):

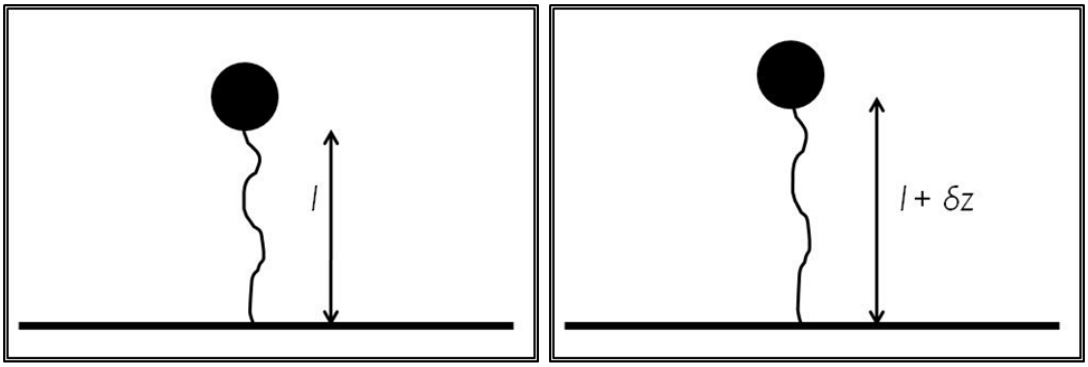

Figure 1.2: Extension of polymer chain in the z-direction

$$\mathrm{F}(l + \delta z) = \mathrm{F}(l) + \left.\frac{\partial \mathrm{F}}{\partial \mathrm{z}}\right|_{l} \cdot \delta \mathrm{z} + \cdots \qquad (1)$$

F represents the polymer entropic restoring force and from the second term in the series, which is the 1st order leading term, we find the longitudinal spring constant to be:

$$h_{\parallel}(z) = \left.\frac{\partial \mathrm{F}}{\partial \mathrm{z}}\right|_{l} \qquad (2)$$

As this spring constant is based on an ideal Hookean model, it is a linear coefficient. In a real system, however, the polymer has a finite contour length and therefore, the spring constant diverges as the extension of the polymer chain approaches its contour length (Figure 1.3). There extension eventually grows quickly with a steep gradient, as more force is applied.

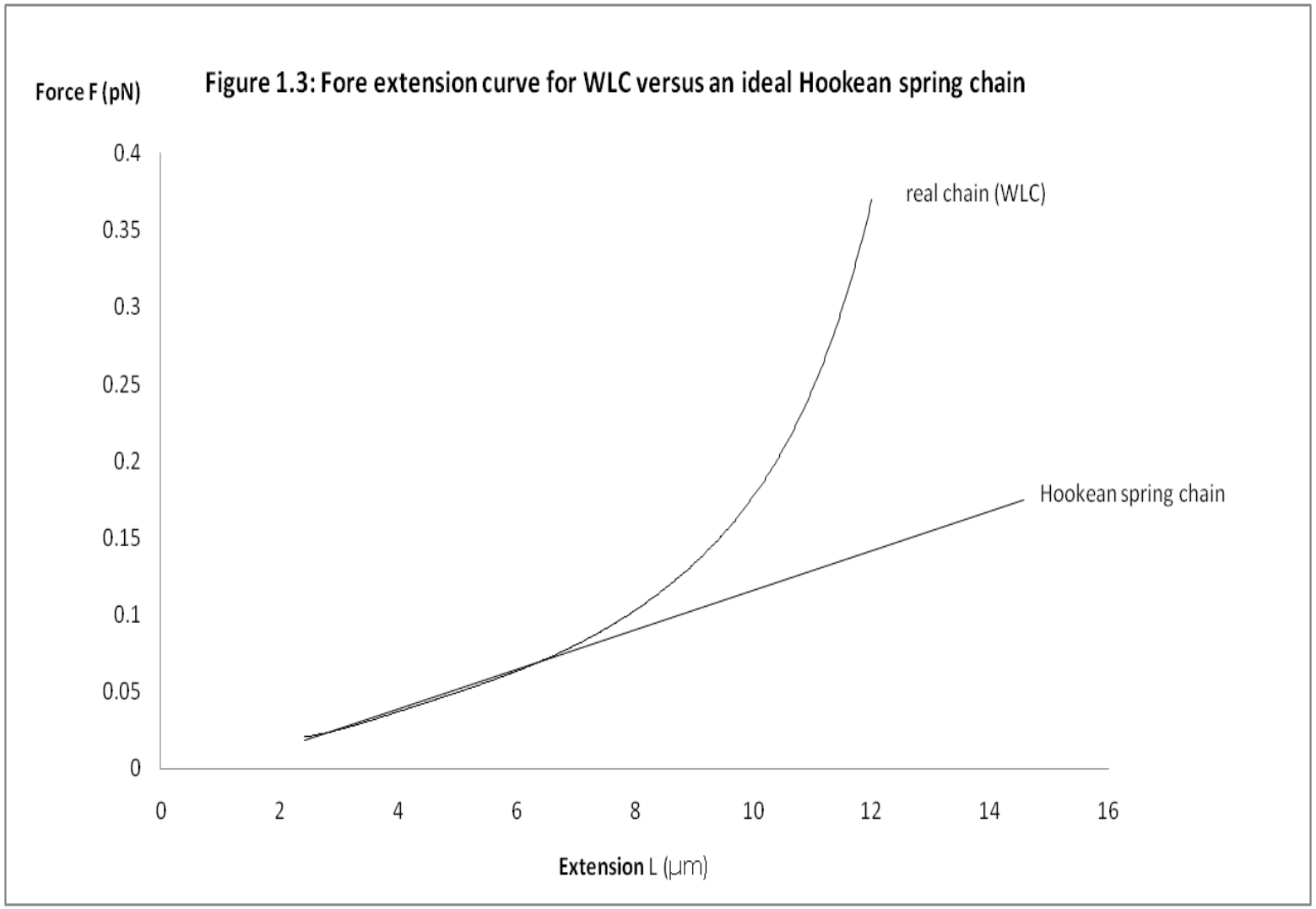

Figure 1.3: Fore extension curve for WLC versus an ideal Hookean spring chain

The transverse spring constant is related to thermal fluctuations of the bead tethered to the polymer chain in either the x-axis or y-axis.

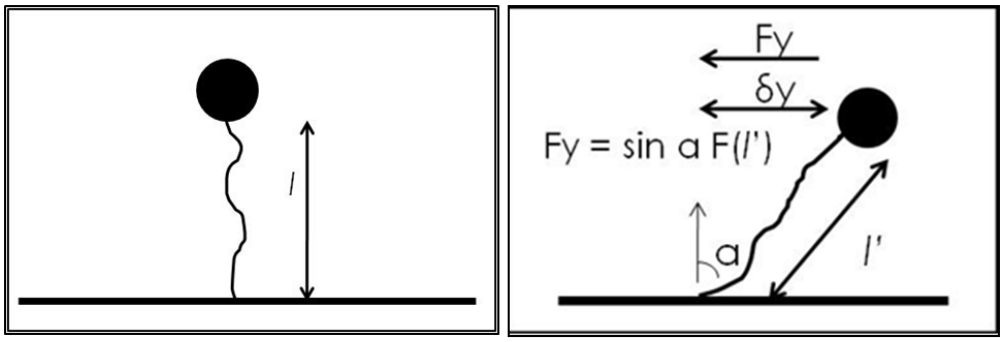

Figure 1.4 Extension of polymer chain in the y-direction

Bead displacement on both directions, which should take a Gaussian distribution, should ideally be identical and therefore, the spring constant will be identical as well. This fluctuation, unlike the fluctuation in the z-axis direction, causes considerable change to the extension of the polymer and using the trigonometric properties, the change in length, l' is:

$$l' = \sqrt{l^2 + \delta y^2} \tag{3}$$

Therefore, the polymer entropic restoring force in the y-axis direction is given as:

$$\mathrm{F}_y = \sin\alpha \cdot \mathrm{F}(l') \tag{4}$$

$$\mathrm{F}_y = \frac{\delta y}{\sqrt{l^2 + \delta y^2}} \cdot \mathrm{F}\left(\sqrt{l^2 + \delta y^2}\right) \tag{5}$$

Assuming that the total contour length of the polymer chain is considerably greater than the fluctuation (l >> δy):

$$\mathrm{F}_y \cong \frac{\delta y}{l} \cdot \mathrm{F}(l) \tag{6}$$

Changing the order of the terms in equation (6), we find the transverse constant to be:

$$h_{\perp}(y) = \frac{F(l)}{l} \tag{7}$$

The energy balance, which is in relation with the magnitude of the transverse thermal fluctuation of the bead tethered to the polymer chain, is another term that should be considered in order to calculate the force on this system. Based on the Equipartition theorem [26], motion of the bead is induced by the thermal energy, and this is balanced by the diffusion of the bead in a potential well:

$$E^{d} = \frac{1}{2}\, h_{\perp}\langle {\delta_y}^2 \rangle \tag{8}$$

$$E^{thermal} = \frac{1}{2}\, k_B T \tag{9}$$

$$\frac{1}{2}\, k_B T = \frac{1}{2}\, h_{\perp}\langle {\delta_y}^2 \rangle \tag{10}$$

Rearranging the equations and using equation (7) results in the following equation that shows the relationship between force and other related terms that can be measured:

$$F(l) = \frac{k_{\boldsymbol{B}} T\, l}{\langle {\delta_y}^2 \rangle} \tag{11}$$

The final derivation shows that measurement of the extension l and the mean square displacement of the particle $\langle {\delta_y}^2 \rangle$ from the experiment allows us to calculate the force exerted on the polymer chain.

1.4 Lambda-phage DNA

The polymer used in this experiment is lambda-phage DNA, a readily available and widely used piece of double stranded DNA (dsDNA). Lambda-phage DNA is isolated from bacteriophage lambda of *Escherichia coli* (*E.coli)*. It is a well characterized long piece of polymer that has been used prevalently by many research groups due to its easy availability, which makes it a good initial platform to perform initial experiments on and to optimize the conditions for the experimental set up and the analysis method.

Lambda-phage DNA is dsDNA that is 48,502 base pairs long, corresponding to 16.3 µm in length. Its double helical structure leads to a rigid backbone [27, 28], which makes it a semi-flexible polymer, and therefore can also be described by the wormlike chain model (WLC).. A semi-flexible polymer is defined as chains connected by multiple bonds that have the tendency of making the backbone continue in a given direction [29]. Polymers that are classified under semi flexible polymers have persistence lengths that can be described by the following equation [29]:

$$l_p = \frac{l}{1-\propto} \qquad (12)$$

where *lp* is the persistence length, and *l* is the length of each bond, and α = cos Θ. Persistence length is defined as "a measure of how far along the backbone one has to go before the orientation changes appreciably" [29]. DsDNA has a long persistence length of approximately 53nm, characteristic of semi-flexible polymers. Semi flexible polymers can still bend and entangle, but do not coil up or collapse as would flexible polymers. Semi

flexible polymers therefore can be depicted as linear elastic rods, with more freedom on short scales and more rigidity in long scales.

The semi-flexible polymers defer from flexible polymers in that flexible polymers have shorter persistence lengths and they therefore move with more random motion and has higher degree of freedom. The persistence length of a flexible polymer differs from that of a semi-flexible polymer as such [29]:

$$l_p = C_\infty l \qquad (13)$$

where C∞ is the constant value of a measure of chain flexibility for large number of bonds (the Cn value at large n, the number of bonds). Moreover, in order to maintain its flexibility, flexible polymers do not have as many side groups, which could cause bending rigidity and moreover, the side groups will be smaller in size as well to be classified as flexible polymers.

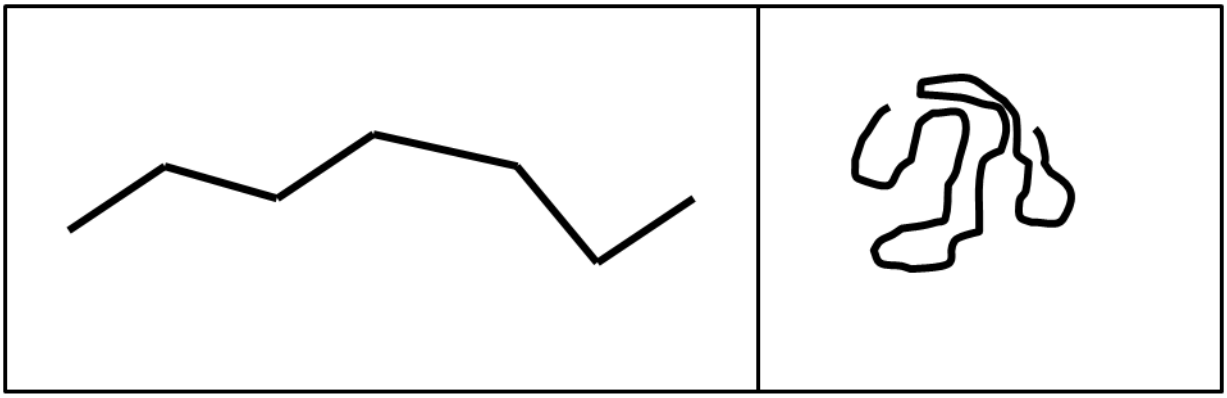

Figure 1.5 semi-flexible polymer and flexible polymer

Chapter 2

Experimental Methods

2.1 Experimental Set Up for Magnetic Tweezers

This chapter describes the preparation steps to make single molecule elasticity measurements using the magnetic tweezers. A flow cell (Figure 2.1) needs to be built, in which the polymer will be incubated to form a tether with a magnetic bead. In order to obtain the two experimental quantities mentioned in the previous chapter, the thermal fluctuation and the extension due to applied force, inverted fluorescence microscope set up is used. Procedures as to how to interpret the experimental data in order to find the applied force is also described.

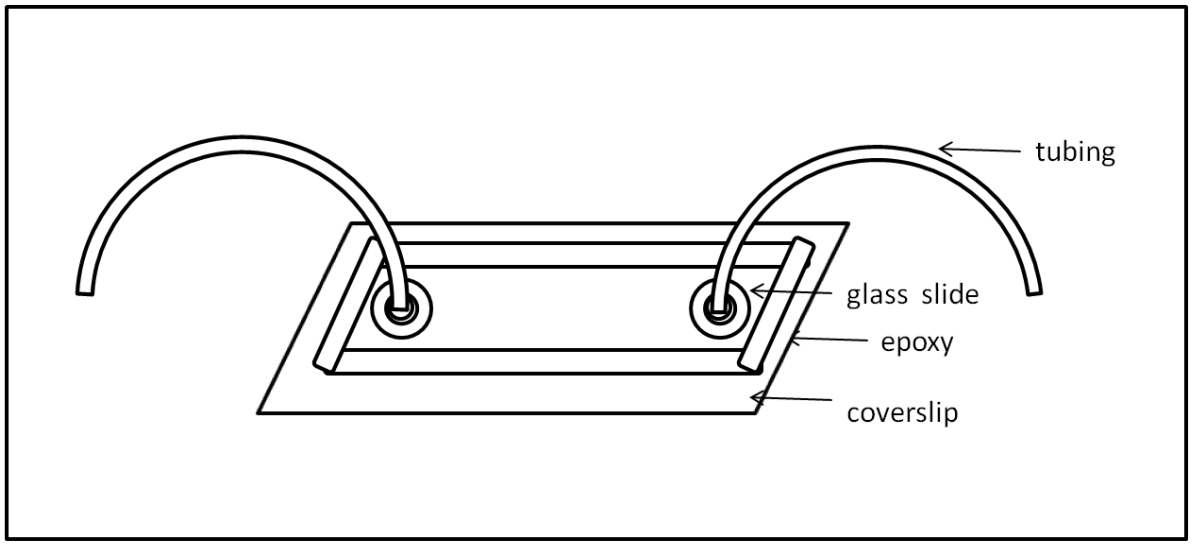

Figure 2.1 Flow cell set up

2.2 Cleaning and Functionalizing Coverslips

Coverslips are cleaned and functionalized on one surface in order to be used in building the flow cell. Twenty 24x60 mm coverslips (Fisher Scientific) are prepared in each batch. For the initial cleaning steps, the coverslips are placed in teflon slide containers, and the containers are first filled with ethanol. The containers are sonicated for 30 minutes. After removing the ethanol, the containers are washed with distilled deionized water ($_{dd}H_2O$), and then the containers are filled with 1 M KOH, and sonicated for another 30 minutes. The above step is repeated twice for a total of three washing steps. After the last sonication step with 1 M KOH, another sonication with ethanol for 30 minutes is required. $_{dd}H_2O$ should be used to wash the containers between each step. After the last sonication with ethanol, the containers are filled with acetone and sonicated for 15 minutes.

During the final sonication step with acetone, a 500 ml beaker should be prepared, fully scrubbed and washed with dish soap. The beaker should be thoroughly rinsed with tap water, then $_{dd}H_2O$, and then finally with acetone. Once it is washed, the beaker is filled with 300 ml acetone, and 6 ml of (3-aminopropyl) triethoxysilane using a glass pipette is added and mixed. The solution is poured into the coverslip containers and the containers are set at room temperature without sonication for 5 minutes. This allows the coverslip to react with Si on the (3-aminopropyl) triethoxysilane and results in a surface covered with amino groups. The containers are placed in a plastic basin and $_{dd}H_2O$ is poured into the containers to quench the reaction until the containers are rinsed with excess $_{dd}H_2O$. Next, each coverslip is rinsed with a gentle stream of $_{dd}H_2O$, using a pair of plastic end tweezers. Direct flow of

$_{dd}H_2O$ onto the coverslip should be avoided during this process in order for the amino-silylated surface to be unaltered. After the coverslips are washed, they should be placed on aluminum foil and air-dried. This step creates a silanized coverslip surface on to which biotin linked NHS-PEG complex can bind.

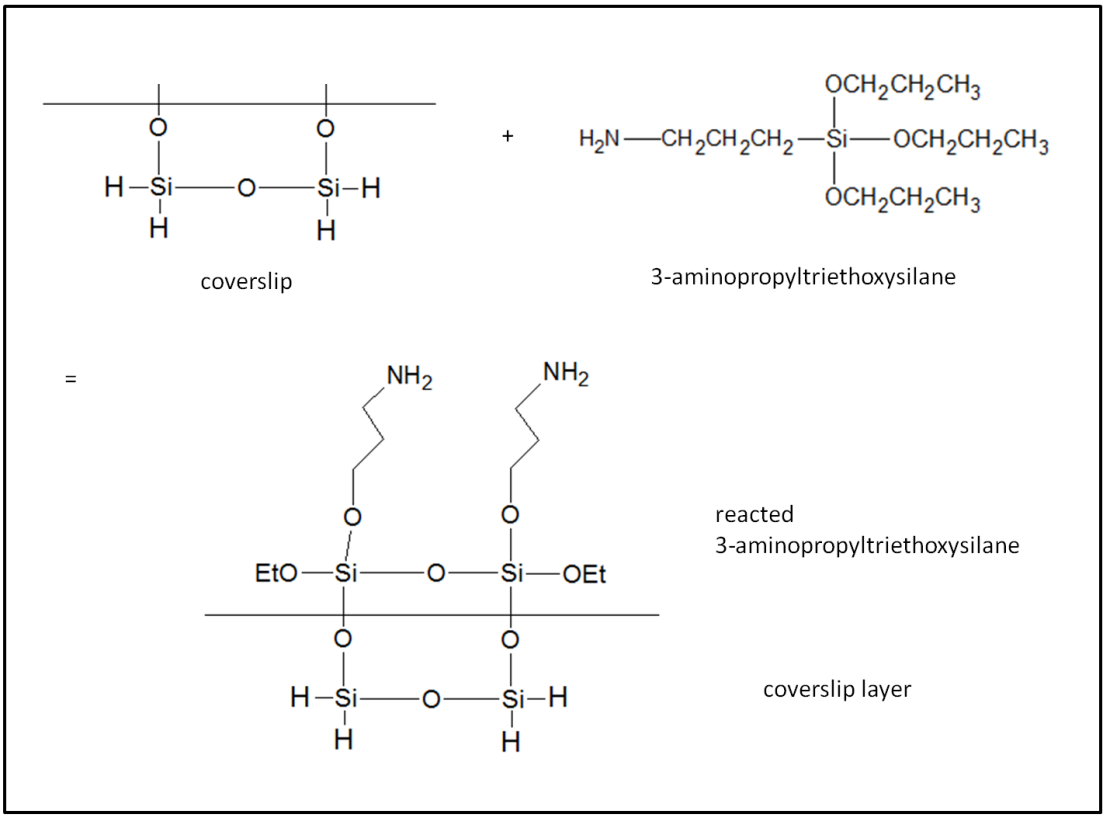

Figure 2.2 Silanized coverslip

After the coverslips are dried, a solution containing 1 ml of 0.1 M sodium bicarbonate and 1 mg of biotin-PEG-NHS in solid powder form should be prepared, mixing the tube only by inversion. Biotin-PEG-NHS, which is normally stored in -20°C in a glass bottle, should be degassed first, purged with N_2 gas and then should be sealed with parafilm around the edges, each time the bottle is opened. This ensures that the extremely reactive

Bioin-PEG-NHS complex to be reused without any loss of reactivity. Coverslip sandwiches, as shown in the (figure 2.3) are built, so that primary amine groups on the coverslips can react with N-hydroxysuccinimide ester (NHS) from biotin-PEG-NHS and form amide bonds (figure 2.4). One coverslip is placed onto a plastic box with two 22x22x0.18 mm coverslips (Fisher Scientific) on each end as spacers, and 100 µl of the biotin-PEG-NHS solution is pipetted onto the coverslip. Next, another coverslip is sandwiched onto the spacers, which allows the biotin-PEG-NHS solution to spread between the coverslips and allow the reaction to proceed on both surfaces. The reaction proceeds for three hours at room temperature and then, each coverslip is rinsed with $_{dd}H_2O$, without the flowing water directly flowing onto the reacted side of the coverslips. The coverslips are fully dried using air or N_2, and stored in vacuum until they are needed for future experiments.

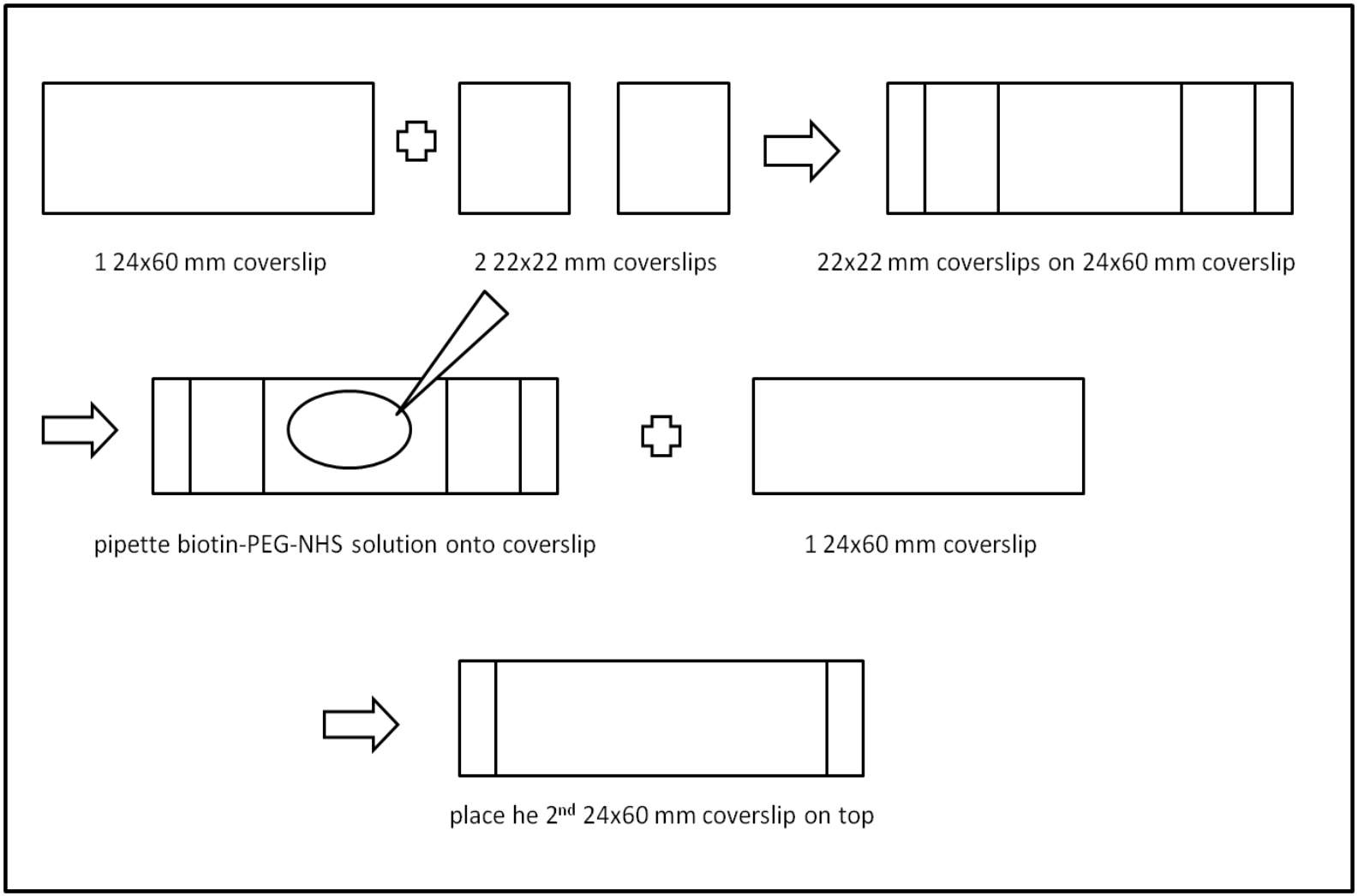

Figure 2.3 Building coverslip sandwich for surface functionalization

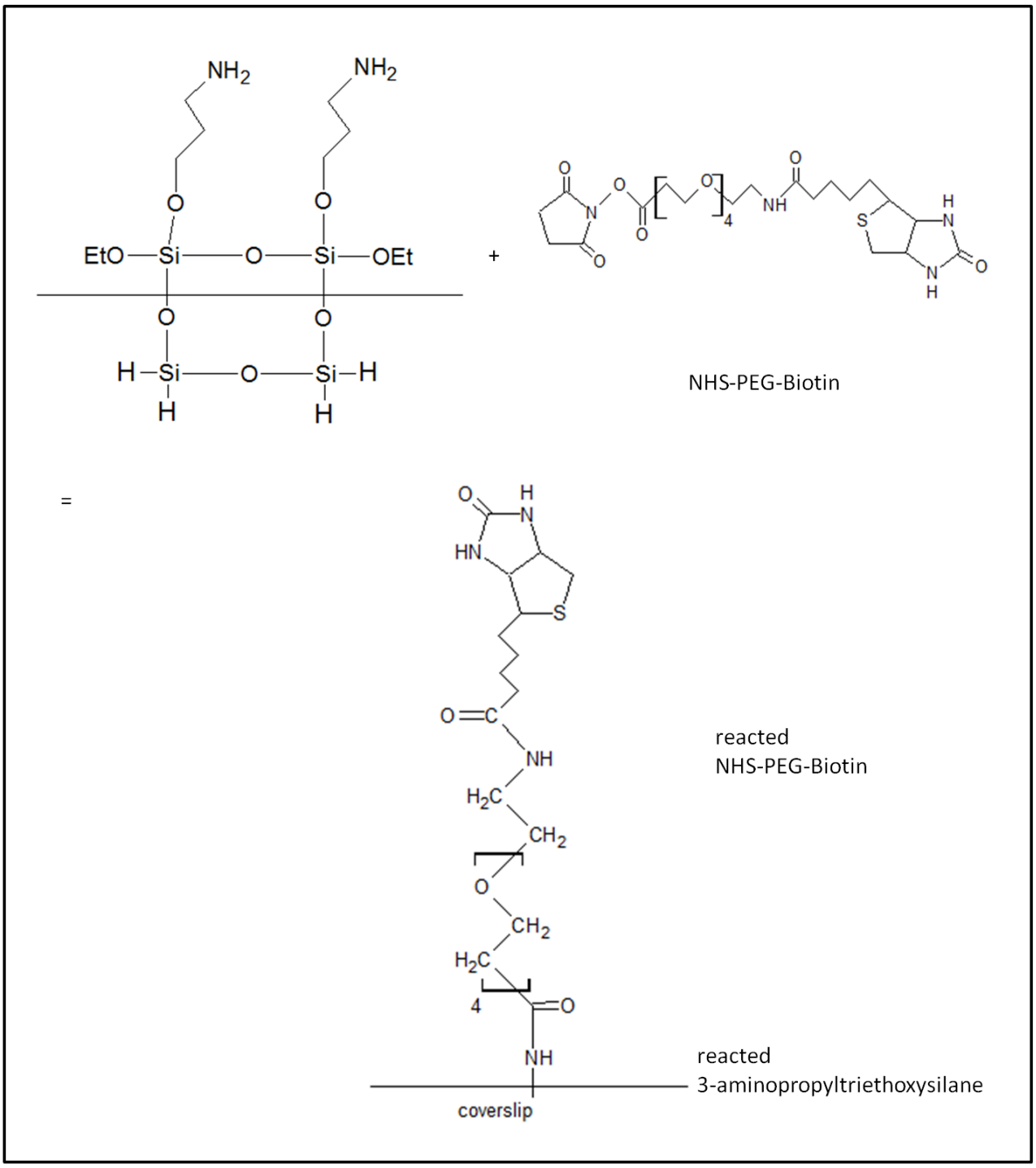

Figure 2.4 Coverslip functionalized with NHS-PEG-Biotin

2.3 End-labeling Lambda-phage DNA

Lambda-phage DNA (New England Biolabs) isolated from bacterioahage lambda, is functionalized on both ends to facilitate single molecule experiments. As shown in Figure 2.5, a linker oligonucleotide is hybridized onto the 5' overhang of the lambda-phage DNA and subsequently ligated to the 3' terminus on the same end. Overall, this scheme allows both biotin and DIG linker oligonucleotides to be ligated onto the same strand on the double stranded lambda-phage DNA. The linker oligonucleotide is diluted to a concentration of 100 µM. 50 µl of lambda-phage DNA (at 500 µg/ml), 5.5 µl of 10x T4 DNA ligase buffer, and 0.5 µl of the diluted linker oligonucleotide at 10 µM is mixed, heated to 70°C for 2 minutes on a heating block, and allowed to cool down to room temperature on the heating block for annealing. Once the mixture has reached room temperature, 15 µl of 10x T4 DNA ligase buffer, 127 µl of $_{dd}H_2O$ and 2 µl of T4 DNA ligase is added to the above annealed linker mixture and the reaction is run for 3 hours at room temperature for ligation.

Once the above mixture has been prepared, two oligonucleotides, one with TEG-biotin end and the other with DIG-NHS end, are annealed and ligated onto the lambda-phage DNA. Stock oligonucleotides are mixed with $_{dd}H_2O$ to achieve 100 µM each, and 2 µl of each oligonucleotide solutions (further diluted to 10 µM) are added to the mixture containing the lambda-phage DNA with a ligated linker oligo. As in the above reaction, the mixture is set on the heat block at 70°C for 2 minutes and allowed to cool down to room temperature for annealing. Next, 60 µl of 10X T4 DNA ligase buffer, 540 µl of $_{dd}H_2O$, and 4 µl of T4 DNA ligase is mixed into the tube, and final mixture is set at room temperature

overnight for the final ligation step. This process yields the final functionalized lambda-phage DNA shown in the figure at a concentration of 1.1 nM.

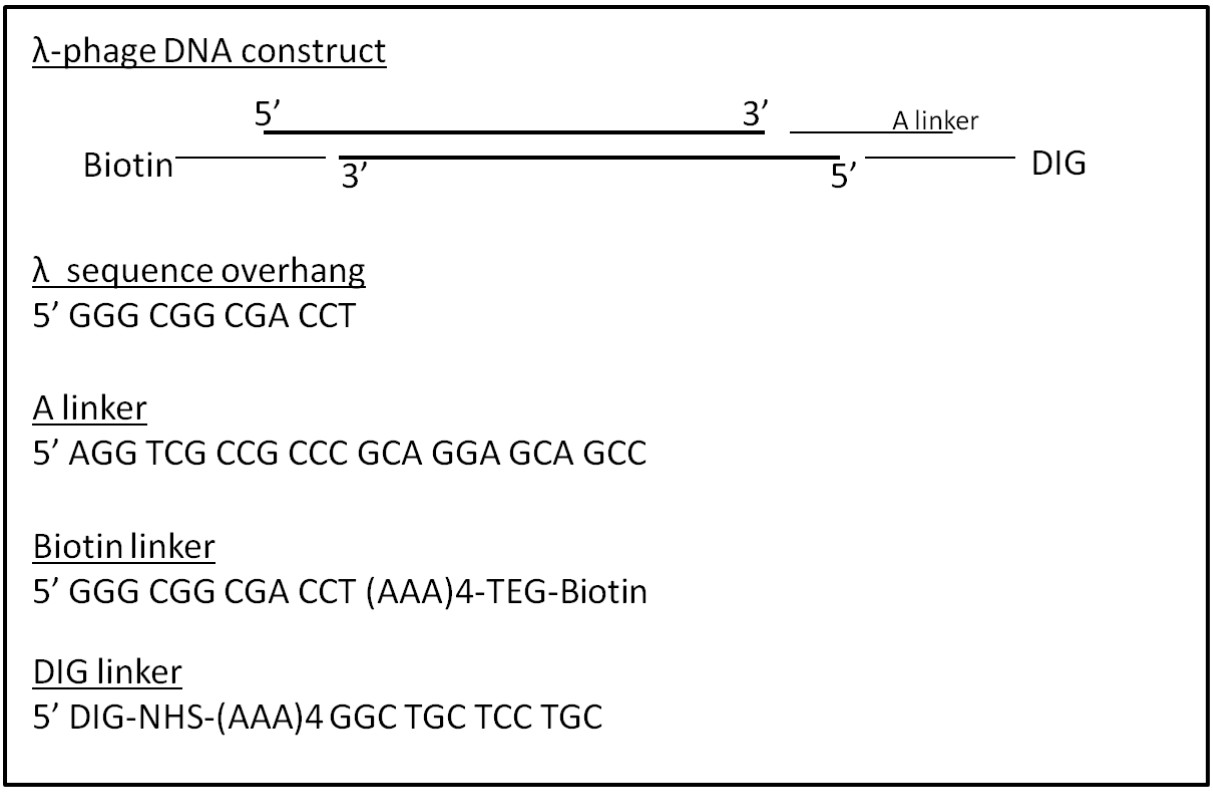

Figure 2.5 Functionalized λ-phage DNA and the sequences of the linkers

2.4 Functionalizing Magnetic Beads

2.8 µm diameter Dynabeads (M-270 carboxylic acid, Invitrogen) are functionalized with Anti-DIG to facilitate coupling with DIG that is functionalized at one end of the prepared lambda-phage DNA. First, the beads are rinsed to prepare the surface for reaction. 100 µl of 25 mM MES (2-(N-morpholino)ethanesulfonic acid) buffer (pH 6.0) is added to 100 µl of Dynabeads, and the mixture is mixed at room temperature via slow rotation for ten

minutes. As the beads in the stock bottle are settled down to the bottom, the bottle should always be mixed using light vortexing before taking the beads out of the stock bottle. Proper mixing ensures that the accurate concentration of the stock bead solution is used. After drawing down the beads with a magnet, the supernatant should be carefully removed by pipetting. The bead cleaning step is repeated twice. After the cleaning is done, 200 µl of MES buffer is added and the tube is set on ice until needed. EDC/NHS solution is prepared by making 50 mg/ml solutions of NHS (N-hydroxysuccinimide) and EDC (1-ethyl-3-(3-dimethylaminopropyl) carbodiimide) separately with the MES buffer. The two solutions are each mixed separately in a tube by inversion and kept on ice. After the EDC and NHS solutions are prepared, the supernatant from the bead solution is removed while pulling down the beads with a magnet, and 50 µl each of the EDC and NHS solutions are added to the tube with the beads, mixed by pipette, and also mixed briefly using vortex. The tube is mixed by slow tilting at room temperature for 30 minutes to allow the beads to be fully dissolved in the solution.

While the above reaction is proceeding, 1mg of Anti-Digoxigenin (Roche Applied Science) is removed and mixed with 400 µl of 25 mM MES buffer to yield a 2.5 mg/ml solution. When the bead solution is mixed, the supernatant is removed and is rinsed with cold MES buffer twice, as in the initial cleaning step. Then, 60 µl of the Anti-DIG solution is added, immediately followed by addition of 40 µl of 25 mM MES buffer. The solution is mixed by pipette and gentle tapping, and then the tube should undergo the slow tilting process at room temperature for 90 minutes. When the above reaction has terminated, the

supernantant is removed and 200 µl of quenching buffer (50 mM Tris, 200 mM NaCl, 10% glycerol) is added and mixed by pipette to stop the reaction. The mixture is slowly rotated at room temperature again for 60 minutes. The remainder of the Anti-DIG solution is stable between -15°C and -25°C and therefore should be stored in the -20°C freezer.

When the above reaction has terminated, the supernatant is removed and the beads are washed with 200 µl of washing solution (10 mM phosphate buffer, 200 mM NaCl, 0.2% Tween 20, 1 mM EDTA, 10% glycerol, 0.0005% sodium azide) 4 times repeatedly. When the beads are thoroughly washed, the supernatant is removed and 1 ml of the wash buffer is added to the beads. The final solution is vortexed for approximately 30 seconds and the solution is stored at 4°C in aliquots of 100 µl.

2.5 Building a Flow Cell

To build a flow cell, a glass slide is cut to the desired size (approximately 51 x 20 mm) and two 1.25 mm diameter holes are drilled into the glass slide, using standard diamond drill bits (Kingsley North Inc.) and a rotary tool (DREMEL) so that the sterilized tubing can be connected as inlets and outlets to allow solutions to flow through. The drilled holes need to be far enough apart for the magnets to fit in between the two tube lines. The magnets and the housing for the magnets have an outer diameter of 1.00''. On the day of the experiment, double- sided sticky tape is cut to the size of the glass slide, and a flow line (approximately 4mm in width and 2mm longer in length from the drilled holes on each side) is cut out using a clean razor blade. One side of the tape with the paper cover is attached to a clean glass

slide that is rinsed with ethanol in advance. One of the PEGylated coverslips that was stored in vacuum is incubated with 1 mg/ml of NeutrAvidin (Pierce) for 5 minutes on a flat surface. NeutrAvidin is stored at -80°C in aliquots of 500 µl, and 100 µl of the stock aliquot is mixed with 100 µl of TE50 buffer and 2 µl of 1% Triton. NeutrAvidin is a tetrameric protein that has strong affinity to biotin and therefore will form a bond with biotin linked to the surface of the functionalized coverslip. The coverslip is rinsed with $_{dd}H_2O$ without direct or quick flow onto the surface. The coverslip is then blown dry with N_2 or air. The functionalized side of the coverslip is attached to the glass slide and the double-sided sticky tape, and the exposed edges are completely sealed using 5 minute epoxy. The polyethylene tubing (INTRAMEDIC) with ends cut at an angle are placed carefully into the holes punched in the glass slide, and the flow lines are fixed into the flow cell with epoxy. To ensure that no clogging occurs, the epoxy should be added around the tubing when it is slightly dry, so that it does not get flown into the holes. Moreover, to ensure that there is no leakage in the flow cell, the double-sided sticky tape should be stuck fully on both the glass side and the coverslip. This can be accomplished by pressing down on the double-sided sticky tape onto the glass slide at first with a pipette tip, then pressing down the coverslip onto the glass slide that has the double-sided sticky tape applied, also with a pipette tip. Applying too high a pressure onto the coverslip with the pipette tip can cause it to crack, so this procedure should proceed with caution. Figure 2.1 shows a fully built flow cell set up.

2.6 Experimental Set-up on Inverted Microscope

When the epoxy around the glass slide and the tubing are fully dry, the flow cell is set on an inverted microscope. The inlet tubing is submerged into a 15ml tube containing approximately 10 ml of blocking buffer (100 mM phosphate buffer at pH 7.5, 300 mM NaCl, 5 mM EDTA, 0.1% Tween 20, 0.05% sodium azide, 0.1% BSA, 0.1% RNA (from torula yeast, Sigma Aldrich), 10 wt% glycerol). The outlet is connected to a 3 ml syringe (BD) on a syringe pump (Harvard Apparatus) with a T-valve in between the tubing and the syringe allowing for full control of the flow and to decrease the influence of backflow and pressure. The buffer is introduced at a rate of 300 µl/hr rate using the pump to check for leakage. At this point, care should be taken to ensure no air bubbles in the flow and to ensure that no part of the flow line becomes dry to guarantee a favorable and successful experimental environment. When all the tubes and the syringe are filled with the blocking buffer, the 7.7 µm reference beads (Spherotech, biotin polystyrene particles) at a concentration of 0.125 µg/µl are introduced in at 200 µl/hr.

When the beads begin to enter the flow cell, the flow rate is slowed down to 100 µl/hr in order to induce binding of the biotin coated beads with NeutrAvidin. When the field of view has a desired coverage of the reference beads, the excess beads are washed away with the blocking buffer at a flow rate of 300 µl/hr. The T-valve on the outlet should always be closed when changing the solution that is being supplied on the inlet, which keeps the tethers from being perturbed. Moreover, the opening and closing of the T-valve should be done slowly so that there is as little backflow as possible. After the field is washed,

functionalized lambda-phage DNA at a concentration of 2.2 pM is introduced in at 200 µl/hr and when the solution has entered the flow line, the lambda DNA is incubated for an hour to ensure binding of biotin labeled end of the lambda-phage DNA with NeutrAvidin. The excess functionalized lambda-phage DNA strands are then washed out using the blocking buffer at a flow rate of 300 µl/hr. The functionalized Dynabeads at a concentration of 3.3 fM are then introduced at 300 µl/hr and the flow rate is slowed down to 80 µl/hr when the beads begin to enter the view field, so that the beads functionalized with Anti-DIG can form antibody linkages to the DIG-end of the lambda-phage DNA.

When the beads have covered the field of view sufficiently, the flow is stopped, the T-valve is closed, and the ring shaped magnets (MAGCRAFT) with 1.00'' outer diameter are mounted directly on top of the flow cell so that the magnetic force acting on each bead is equal on all directions, in both the x- and y-axis and so that the magnets are not in the way of the camera and blocking the view. To adjust the magnitude of the magnetic force in the desired range, two to three magnets are used, no more than 20 mm away from the flow cell.

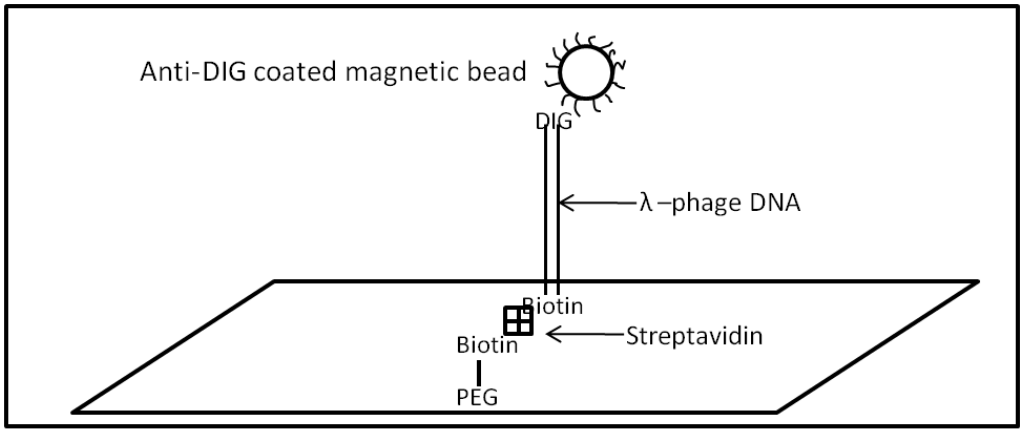

Figure 2.6 Schematic of the complex in the flow cell

2.7 Microscope Set-up

We use an inverted fluorescence microscope (Olympus IX71). Phase contrast technique is used for imaging the beads. Phase contrast is a viewing method that was developed by Frits Zernike, where destructive interference patterns caused by the shifts in amplitude and phase allow more sensitive and clear imaging of the particles against its background [30]. Bright field imaging, another common viewing technique, has been tested as well, but it has shown less optimal view of field in comparison with the phase contrast.

The camera that is used is a back-illuminated Electron Multiplying Charge Coupled Device (EMCCD) camera (Andor ixon+) and this camera shows a 512 x 512 pixel view. The imaging does not require any EM gain and the only light source that is used is the halogen lamp on the illumination pillar of the microscope. Auto-scaling on the magnetic beads is required to obtain an optimal viewing image of the 2.8 μm anti-DIG functionalized magnetic beads in comparison to the larger 7.7 μm reference beads. A 40x phase objective (Olympus, 40x/0.60 Ph2) is used without any additional magnification. With this objective, each pixel is equivalent to 0.4 μm.

2.8 Data Acquisition

An initial image of the view field is acquired taken with the 7.7 μm reference beads in focus, at the beginning of the experiment. The focused ring diameter value of the reference bead corresponds to the y-intercept of the calibration curve that describes the relationship between the ring diameter and the distance of the bead away from the surface.

As this initial y-intercept value is subject to change depending on the experimental set up each day, acquiring the initial image allows us to always calculate distance based on the accurate and relative y-intercept. Both beads should be present in the field of view when recording the videos to ensure accurate measurement (figure 2.7). Next, 600 frame videos at a rate of 30 frames per second are acquired with the 2.8 μm anti-DIG functionalized beads in focus, changing the height of the magnet between each video to induce different magnitudes of force. Each video yields unique extension lengths of the lambda-phage DNA corresponding to different amounts of applied magnetic force. Each video is saved as 16 bit TIFF stacks to be analyzed using Image J and IDL programs. Using the IDL program and the series of codes developed by John Crocker and David Grier [31], the Brownian motion of the tethered beads is calculated. Using the Image J program, the outermost rings around the beads are detected by using the "Find Edges" feature and their diameters determined using the "Analyze Particles" feature. The ring diameter is used to measure the length of extension of the lambda-phage DNA.

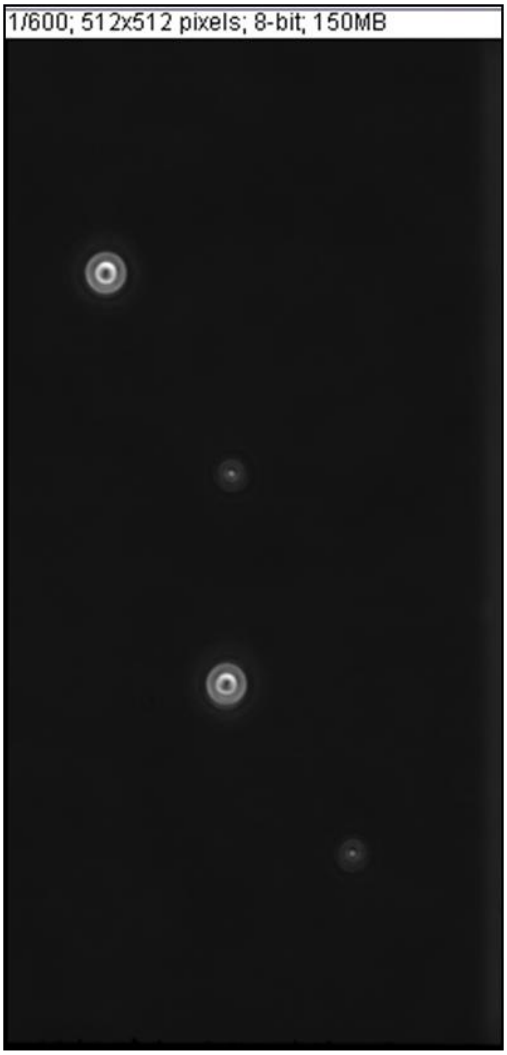

Figure 2.7 Imaging with 2.8 µm and 7.7 µm beads

2.9 Calibration Curve for Extension Measurements

Calibration curves are prepared using the 7.7 µm diameter reference beads. A glass slide- coverslip sandwich is prepared so that the reference beads are immobilized on the coverslip surface. The coverslip is first attached to a glass slide with double sided tape on two ends. Next, a solution containing 996 µl TE50 buffer, 2 µl 1 M HCl and 2 µl of reference beads is prepared and introduced into the cell by pipette using the osmotic effect. The

solution is allowed to incubate for 5 minutes, so that the beads can stick to the surfaces. The solution is then removed by flowing in excess TE50 buffer, and all four ends of the cell area are sealed using epoxy to prevent the incubated cell from drying out (figure 2.8).

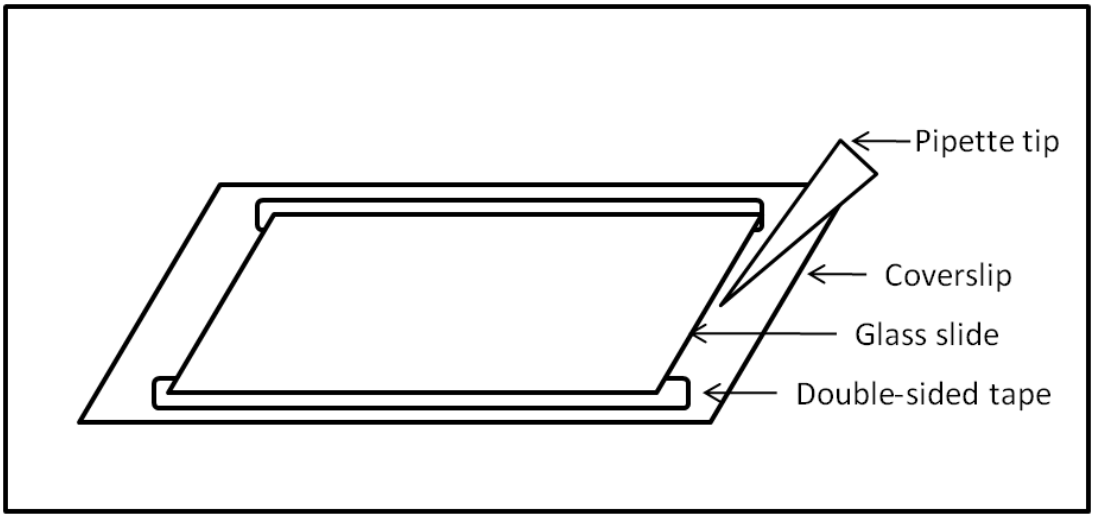

Figure 2.8 Coverslip glass slide sandwich for calibration measurements

A piezo stage (Physik Instrumente) that can move in the z-axis is placed onto the inverted fluorescence microscope with the customized adapter plate (consisting of anodized aluminum to prevent magnetic interactions). For calibration measurements, a bifocal lens (Thorlabs, D = 25.4 mm, F = 100.0 mm) is inserted into the cassette (DV2-CUBE, 630dcxr) into the short wavelength slot of the dual view (DV2, MAG Biosystems), which shifts the distance at which the image is focused. The view is therefore split into two, where the same image looks focused on one side, and defocused on the other. The dual view is placed in between the microscope and the camera. This shows a dual bifocal image view on the camera, one half showing the view in focus and the other out of focus (figure 2.9). This lens

defocuses the view up to 20 µm, which is ideal for this experiment as it has range that is longer than the total contour length of a lambda-phage DNA, which is 16 µm. This set up allows us to measure the change in the ring diameters around the beads as the piezo stage moves in the z-direction [32].

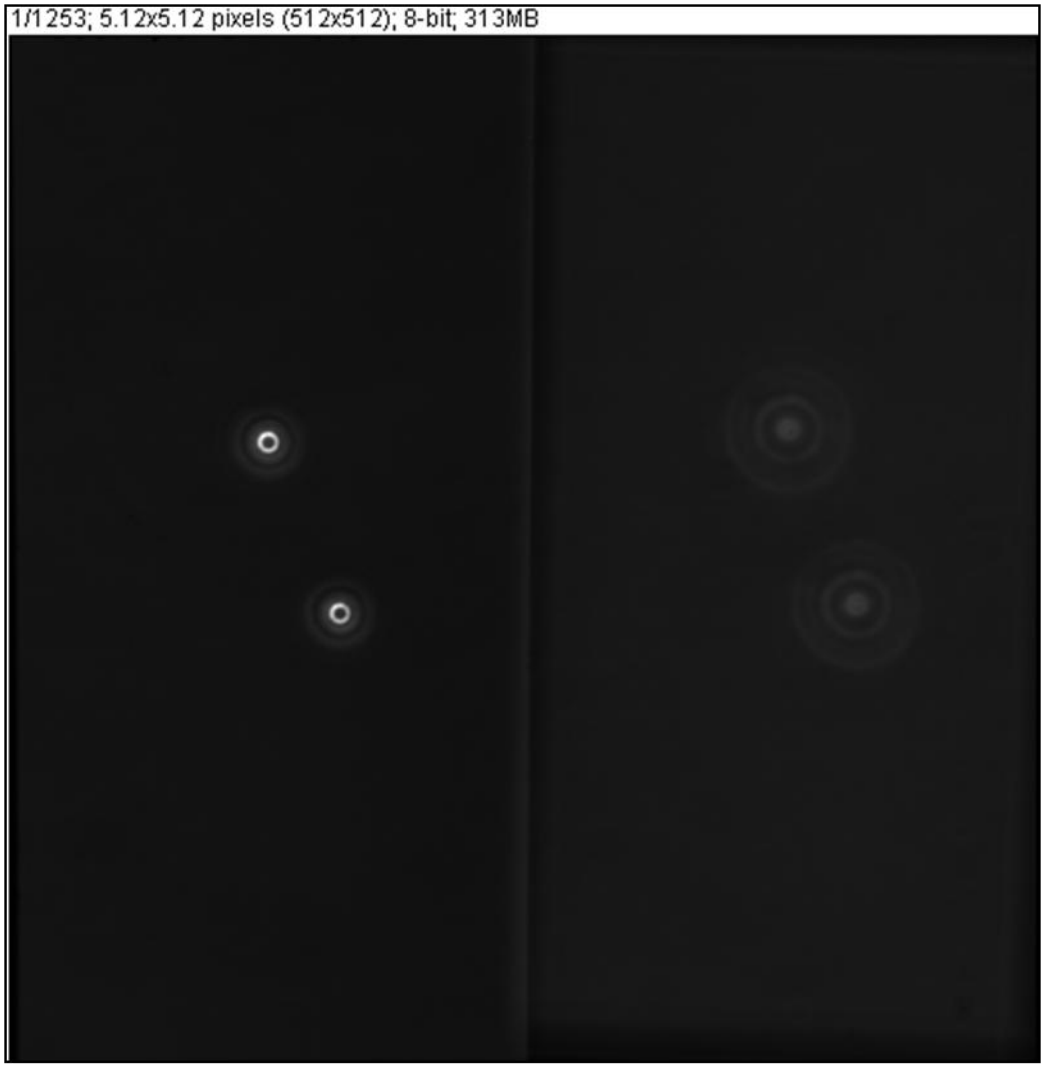

Figure 2.9 Bifocal Imaging of 7.7 µm beads for calibration

The stage is prepared to take 200 nm steps over the range of 20 µm, and 1400 frame videos at 30 frames per second are recorded. The rate is fast enough so that the settling time of 5ms caused by the drift of the piezo stage does not cause considerable affect on the ring patterns around the beads that are recorded in each frame. The ring diameters around the beads on the right-hand size of the image start to become defocused, as those in the left-hand size image start to come into focus, which means the stage is moving upwards, away from the lower surface and into the solution. Overall, this ensures us that when we perform experiments, the ring diameters of the beads become larger as we move away from the coverslip, and into the solution. This means that the ring diameters always increase in size as the extension gets longer. Based on number of total frames and the total number of steps taken, 13 frames are equivalent to each 200nm step. The average value taken from all the diameters of the rings around the beads in these 13 frames yields the ring diameter for 1 step size. It therefore represents a unique value for a certain distance away from the surface, which along with the other values will give us a calibration curve, where the ring diameters increase linearly with distance.

The curve (figure 2.10) shows the ring diameters at each step, which yields a calibration curve that can be used to measure the length of the lambda-phage DNA. The y-intercept could change depending on the experimental set up, but the slope should always be a constant value, regardless of the size of the beads or the change in the size of the initially focused size of the bead.

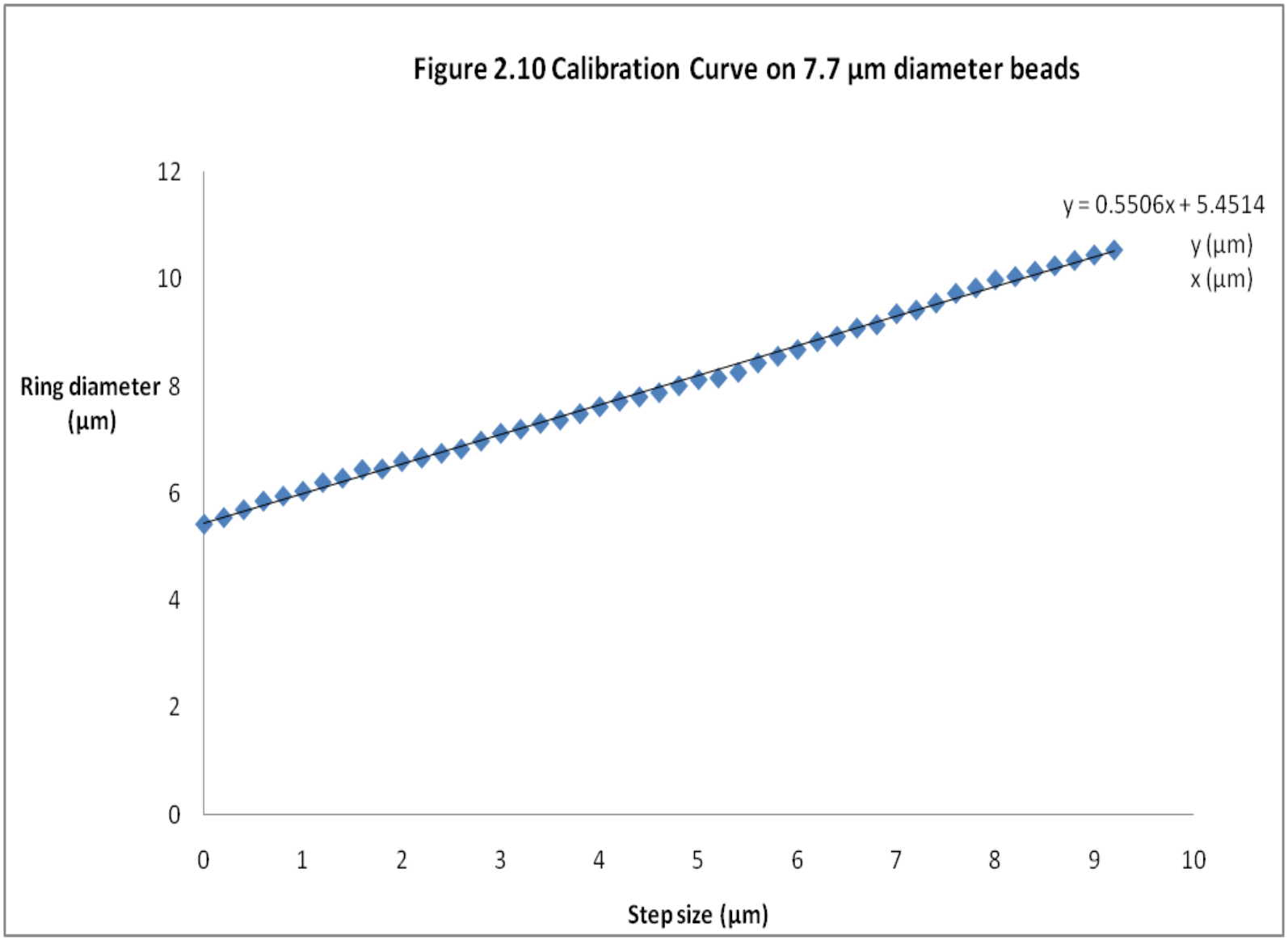
Figure 2.10 Calibration Curve on 7.7 µm diameter beads
y = 0.5506x + 5.4514
y (µm)
x (µm)
Ring diameter (µm)
Step size (µm)
0
2
4
6
8
10
12
0
1
2
3
4
5
6
7
8
9
10

2.10 Image Processing for Force Measurements

When the 16 bit videos are acquired, they are first converted to 8 bit files using the Image J program, so that they are compatible with the codes and built in functions and plug-ins in the IDL and Image J programs. A series of particle tracking and analysis codes developed by John Crocker and David Grier [30] were used to determine the y-directional thermal fluctuation of the magnetic beads tethered to the lambda-phage DNA. The codes locate each bead as particles, and track their positions in each frame in terms of pixels. The code locates each bead by finding its centroid and by determining its higher intensity compared to the surrounding background. For the 40x phase objective used in this experimental set up 1 pixel is equivalent to 0.4 μm. Overall, this analysis procedure yields the trajectories of each bead and therefore their mean square displacement can be calculated, which gives the thermal fluctuation.

The Image J program has a built in plug-in called “Analyze Particles” that allows the users to determine particle diameter and area in terms of pixels. The images that are converted to 8 bit images must also be converted to binary images additionally, in order to run this plug-in. Upper and lower boundaries for values such as intensity, particle size, and circularity were set to optimized values to give the most accurate data for each image file. Ring diameters for all the beads in all 600 frames are averaged, and their relative size is compared to the linear trendline equation of the calibration curve to determine the length of extension. Moreover, as the value of polymer extension obtained from the program inherently includes the bead dimensions as well, δz value (radius of reference bead – radius

of tethered bead) must be subtracted in order to obtain the true extension length of the lambda-phage DNA.

Chapter 3

RESULTS:

MEASURING THE ELASTICITY OF SINGLE BIOPOLYMERS USING MAGNETIC TWEEZERS

3.1 Magnetic Tweezers Results

Using the experimental set up and techniques described in Chapter 2, the elasticity of single biopolymers were measured. The magnetic tweezers experimental results on double stranded lambda-phage DNA were compared with numerical interpolation solution and also to optical tweezers data from the Bustamante group. Potential sources of errors and the outlook of the work and the experimental set up are also discussed.

3.2 Force Extension Curve

Elasticity measurements of single polymers using magnetic tweezers require two experimentally determined quantities to determine the magnitude of force exerted on lambda-phage double stranded DNA: mean square displacement of the bead tethered to the dsDNA and the extension of the dsDNA. The mean square displacement of the bead is obtained by particle tracking and centroid determination of the bead position. The extension of the dsDNA is determined by measuring the outermost ring diameter of the beads. The force is calculated by the relation (Eq. 11) derived in Chapter 1.

Using the procedure described in Chapter 2, the force extension data was obtained (figure 3.1). Data points show that relative extension of the double-stranded lambda-phage

DNA between the range of 15% and 75% was achieved by varying the distance between the magnets and the flow cell, thereby changing the magnetic force exerted on the magnetic bead tethers. As expected for semi-flexible polymers, the force extension curve of a lambda-phage DNA follows the worm like chain (WLC) force relaxation, in accordance with existing theoretical and experimental observations. The characteristic slow increase in extension for forces smaller than the characteristic force kbT/A (=0.08pN for lambda-phage DNA) followed by an abrupt increase in extension as the extension approaches the contour length are both observed [8].

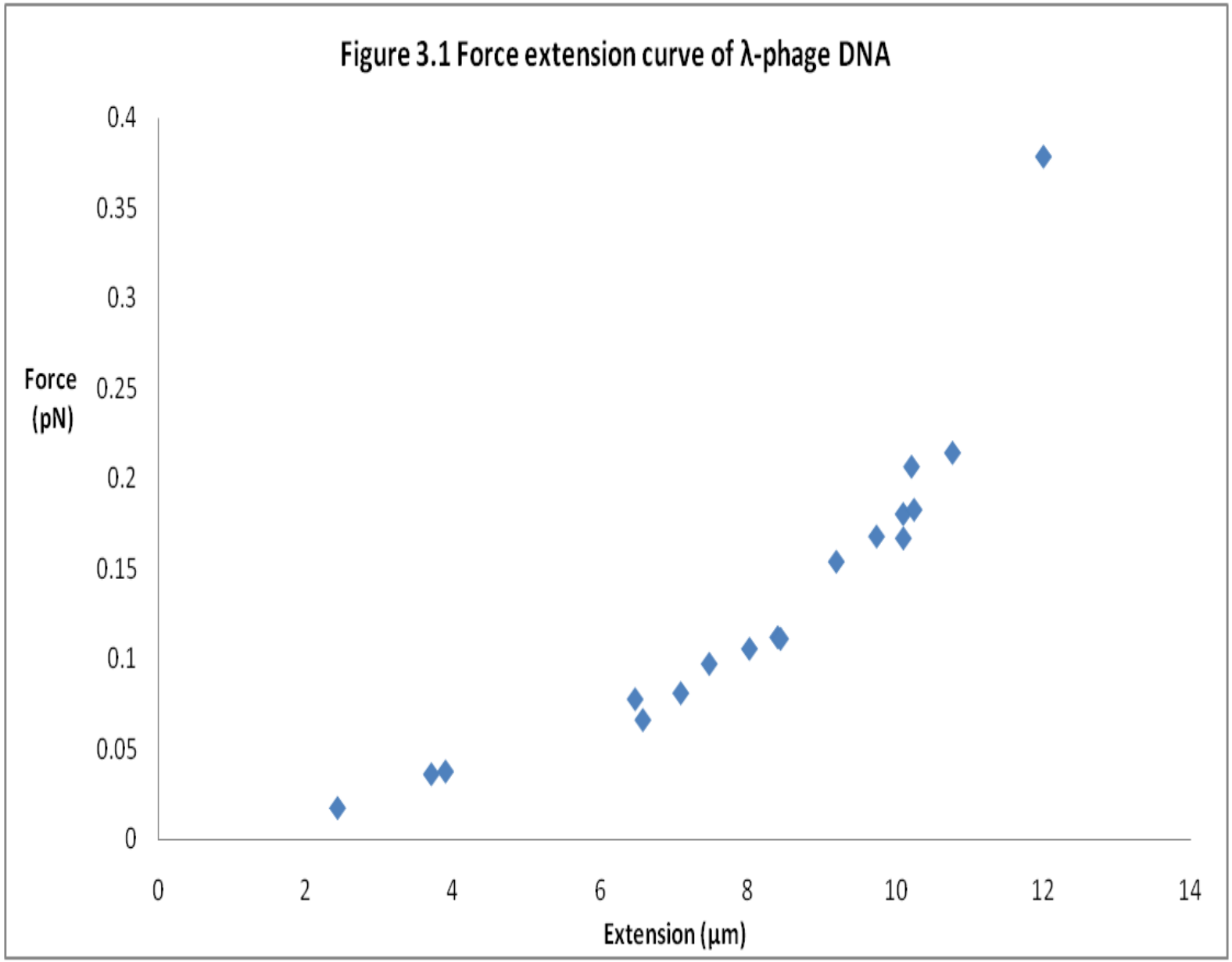
Figure 3.1 Force extension curve of λ-phage DNA
Force (pN)
0.4
0.35
0.3
0.25
0.2
0.15
0.1
0.05
0
0
2
4
6
8
10
12
14
Extension (µm)

The first regime arises because the change in free energy is low when the desired extension z is small compared to the contour length (F = 0.08pN). Therefore, in this regime, the force extension relation may be considered as linear, which suggests that lambda-phage DNA can be modeled as a polymer chain with random walk, where the polymer is an elastic chain with entropy giving rise to the dominant stretching force. As the extension increases beyond this characteristic force, the force extension relationship is no longer linear, and the nonlinear entropic elasticity becomes the dominant contributor to explain the force extension relationship. In this regime, the polymer chain begins to feel the effects of a finite contour length with lower numbers of probably conformations. As a consequence, we observe an abrupt increase in extension with applied force. The polymer chain therefore begins to extend at a much quicker pace, leading to the non-linear regime of the force extension curve.

The force extension curve is also normalized to fit the obtained experimental data to an interpolation solution derived by Marko and Siggia for semi-flexible polymers such as dsDNA (Figure 3.2) [8]. The interpolation solution of Marko and Siggia is also called the worm-like chain (WLC) force relaxation and is given by:

$$\frac{f\mathrm{A}}{k_{\mathbf{B}}\mathrm{T}} = \frac{z}{\mathrm{L}} + \frac{1}{4(1 - z/\mathrm{L})^2} - \frac{1}{4} \qquad (12)$$

where f is the force exerted on the polymer chain, A is the persistence length of the polymer chain in use (A for unstained lambda-phage DNA = 53nm), k_bT is the characteristic thermal energy (= 4.14 x 10^{-21} J at 27 °C), z is the extension of the polymer chain, and L is the contour

length of the polymer chain (L for lambda-phage DNA = 16.3 μm). This equation is applicable to the regime of the force extension curve where the dsDNA is entropically stretched, which is also the regime of the force extension measurements we studied in his experiment. In the nonlinear entropic elasticity regime, the equation is modified as such [22, 33]:

$$\frac{x}{\mathrm{L_0}} = 1 - \frac{1}{2}\left(\frac{k_{\mathbf{B}}\mathrm{T}}{\mathrm{FP}}\right)^{1/2} + \frac{\mathrm{F}}{\mathrm{S}} \qquad (13)$$

where F is the force exerted on the polymer chain, P is the persistence length, and S is the elastic stretch modulus.

The interpolation solution has shown to be a good fit to this experimental data, with error values ranging from 0.87% to 14%, with an average of 6% error. Data for extensions beyond the contour length of the polymer chain were not observed in the experiments.

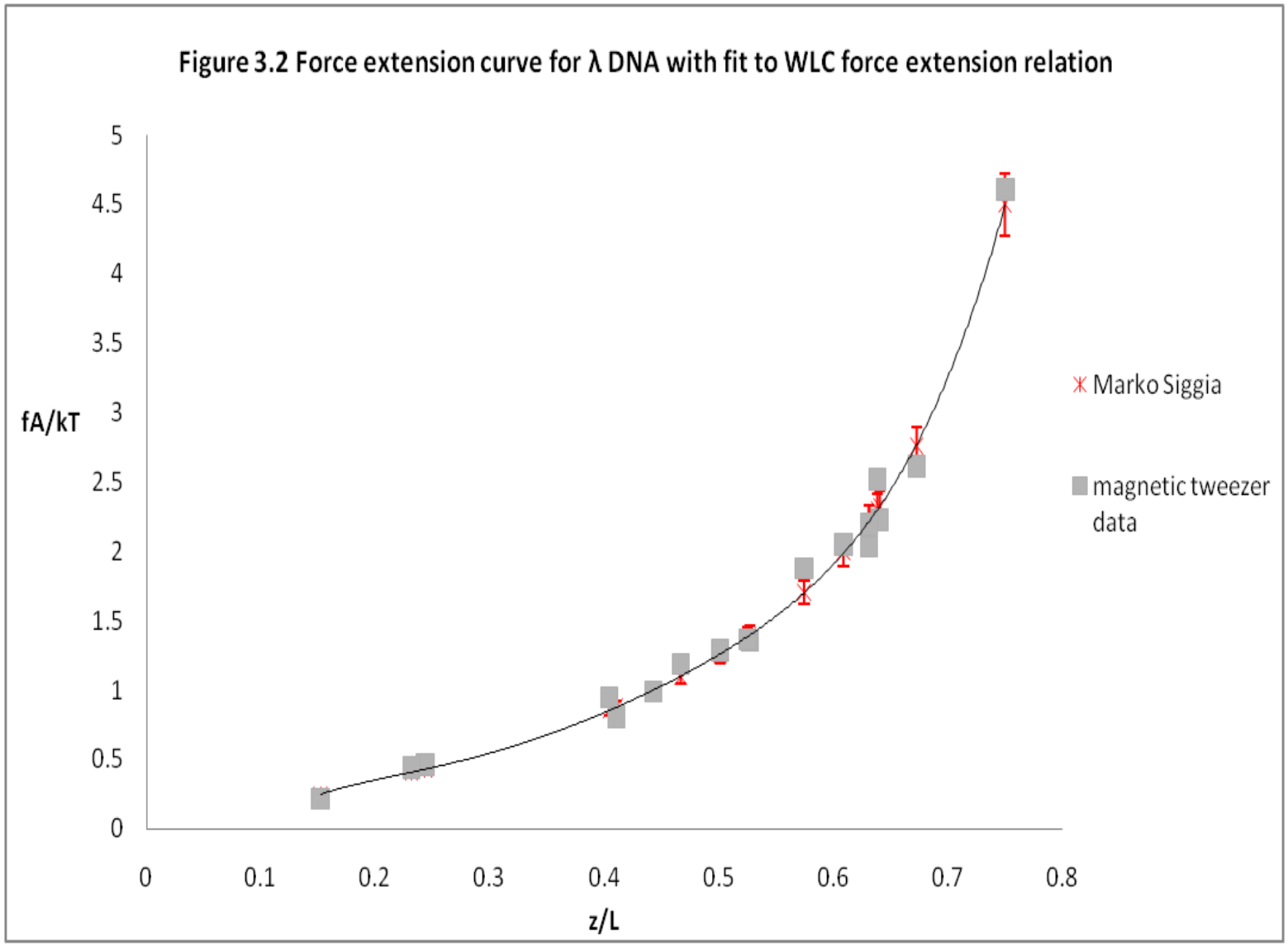
Figure 3.2 Force extension curve for λ DNA with fit to WLC force extension relation
fA/kT
z/L
0
0.5
1
1.5
2
2.5
3
3.5
4
4.5
5
0
0.1
0.2
0.3
0.4
0.5
0.6
0.7
0.8
Marko Siggia
magnetic tweezer data

In addition, experimental values from out magnetic tweezers experiment were compared to an exact solution from experimental data obtained by Smith et al. [10] using optical tweezers (figure 3.3). The experimental data have shown to be a good fit with the data from the Bustamante Group. The interpolation solution of Marko and Siggia has up to 6% error compared to the exact solution from the Smith et al. experiment.

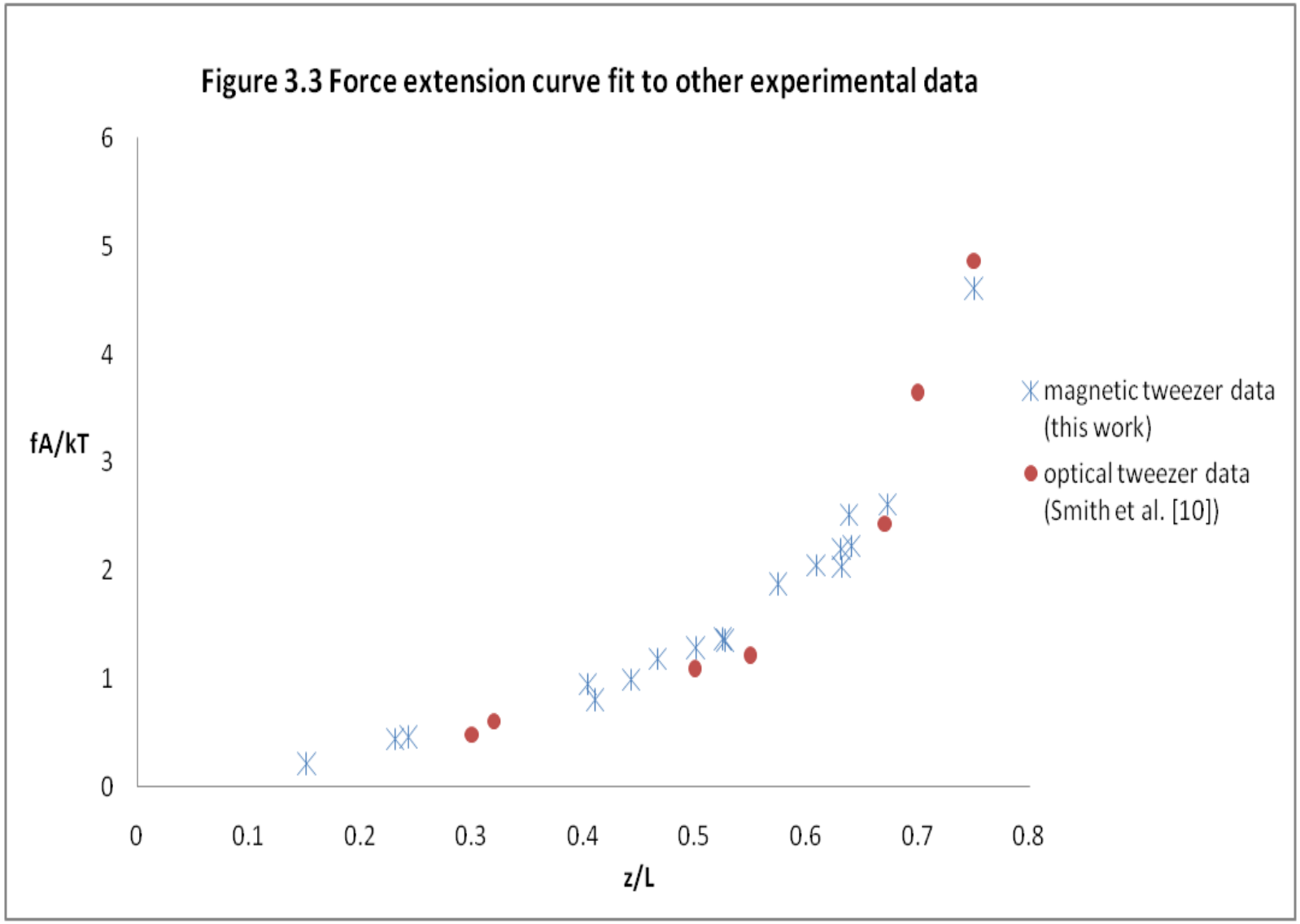
Figure 3.3 Force extension curve fit to other experimental data
fA/kT
z/L
0
1
2
3
4
5
6
0
0.1
0.2
0.3
0.4
0.5
0.6
0.7
0.8
magnetic tweezer data (this work)
optical tweezer data (Smith et al. [10])

3.3 Calibration Curves

Several Potential sources of error were identified in the experiment. Contributions from one or more of these sources may have resulted in increased inaccuracies in determination of the force-extension relaxation for single polymer. First, the piezo stage exhibits a small drift, and the stage has a settling time of 5ms (10% step width), which may have led to errors in the calibration curve.

The calibration curve for determination of polymer stretch was repeated several times and showed that depending on the change in the set up of the incandescent bulb illumination level, approximately 3.5 % of an error can occur for the slope of the calibration curve (figure 3.4). With increased incandescent bulb illumination, the ring diameters around the beads for a given step were shown to be larger as is expected, because more light causes the intensity of the beads to increase, which accentuates the ring structures around the beads. The brightness of the field increases with higher illumination levels and therefore, the ring patterns around the bead become apparent and more prominent. On the other hand, when the illumination is too low, the ring patterns are not prominent. Therefore, there was a minimum and maximum incandescent bulb illumination, only between the range of which reasonable data could be obtained. Although error from the change in illumination is not substantial, the experiments were always performed with equal illumination intensities supplied to the sample flow cell, in order to minimize inaccuracy.

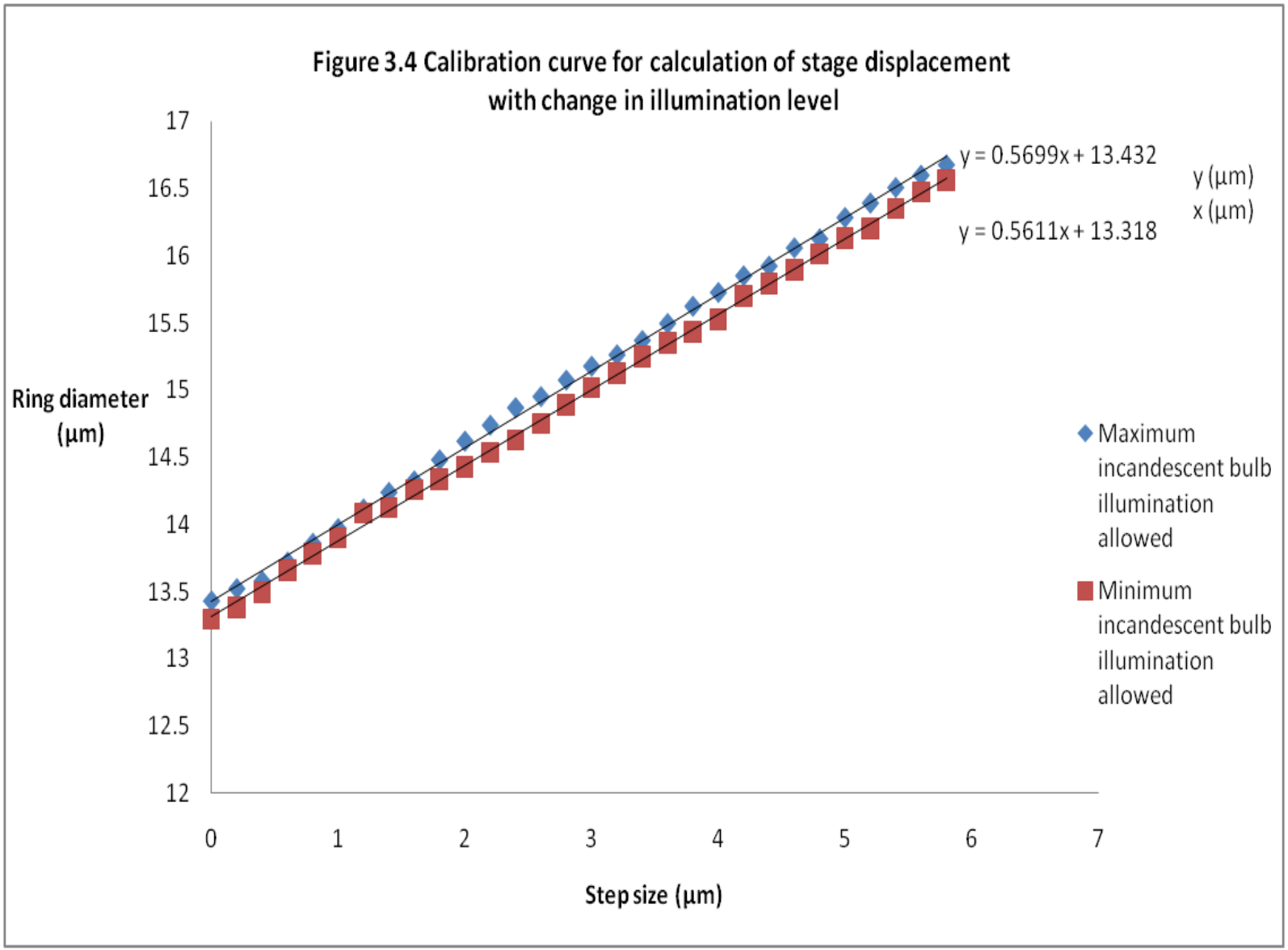
Figure 3.4 Calibration curve for calculation of stage displacement with change in illumination level
Ring diameter (µm)
17
16.5
16
15.5
15
14.5
14
13.5
13
12.5
12
0
1
2
3
4
5
6
7
Step size (µm)
y = 0.5699x + 13.432
y = 0.5611x + 13.318
y (µm)
x (µm)
Maximum incandescent bulb illumination allowed
Minimum incandescent bulb illumination allowed

3.4 Experimental Errors

All the beads appear isotropic in the view field when using the Andor iXon camera. However, because the beads are in thermal fluctuation and the illumination condition varies, the rough edges around the outer ring of the beads can be considered as defects according to the "Analyze Particles" feature in Image J program. The value for the "circularity" parameter in the "Analyze Particles" feature had to be set as low as 60% in some occasions in order for this the program to track particles and find their diameters..

Lambda-phage DNA is stored in the 4°C freezer after it has been functionalized. However, even at 4°C, lambda-phage DNA is likely to degrade due to trace nuclease contamination and can be broken into smaller oligonucleotides. This means that the measurements made on these fragments will give results that are based on strands with different contour lengths, and therefore inaccurate information. To prevent the lambda-phage DNA from degrading, it is stored in -20°C freezer with 50wt% glycerol to prevent solution freezing, within 2 weeks the original date the DNA was functionalized. Degradation in sample can still occur with this precaution and therefore, it is desirable to prepare new samples in regular intervals to ensure success of the experiments. Moreover, using wide-bore pipette tips during handling and mixing processes helps the lambda-phage DNA from experiencing too high a shear rate, which can also cause them to fragment.

Obtaining a perfectly uniform magnetic field in all directions on the tethered magnetic beads is difficult, as the magnets on the stage need to be centered and aligned with respect to the beads. . This would cause a significant error on the thermal fluctuation

and therefore on the mean square displacement of the bead, as the applied force is directly related to how the bead agitates. Such error can lead to shifted and uneven Gaussian curves of the bead displacement. In order to minimize error from non-uniform magnetic field, the magnets have to be perfectly perpendicular to the tethered magnetic beads in the sample flow cell.

Inaccurate data related to thermal fluctuations of the tethered beads can also result in experimental error. This can arise from a small fraction of beads irreversibly adsorbed to the surface, instead of forming tethers with the lambda-phage DNA. Moreover, some beads can be tethered to two or more different lambda-phage DNA strands at a time, resulting from an excess surface coverage of the lambda-phage DNA strands due to increased incubation time, when the lambda-phage DNA is binding to biotin. From the width of the Gaussian curve of each bead, one can determine whether the bead is truly tethered to a single polymer chain or not. If the bead is tethered to a single polymer chain, the width of the Gaussian curve of the thermal fluctuation of the tether spans approximately 4 to 8 pixels, using the imaging set up as described in Chapter 2 (figure 3.5). If the bead is adsorbed to the surface or tethered to multiple strands, the width will either be much narrower or wider. The curve tends to span narrower when the bead has less mobility from being tethered to two different strands, or from being adsorbed irreversibly to the surface. On the other hand, the curve will span wider in width in case where the bead has ill-formed tethers or simply appearing in the view of field without being tethered. Mean square

displacement and extension values from such beads should be omitted when plotting the force extension curve.

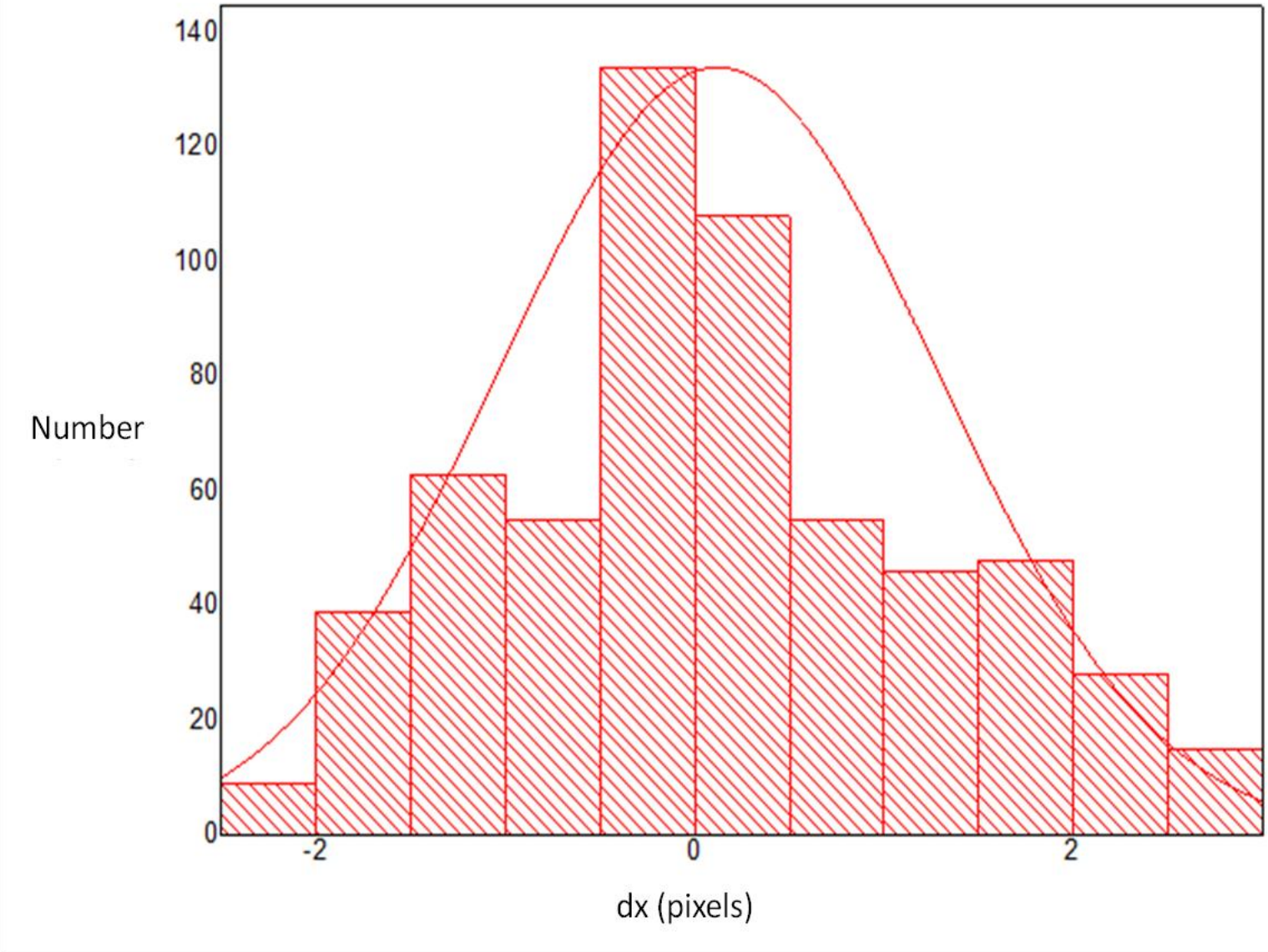

Figure 3.5 Thermal fluctuation of a bead tethered to a single lambda-phage DNA strand

3.5 Outlook

The force extension relationship for single molecules of dsDNA, which is a semi-flexible polymer, was successfully obtained using magnetic tweezers. This experimental set-up can be used to test other novel platforms, such as single stranded DNA strands (ssDNA), synthetic organic polymer chains and polymers with sugar backbones. ssDNA is an interesting platform to be used in single molecule experiments, as it is a truly flexible polymer, unlike the dsDNA which is a semi-flexible polymer. As a flexible polymer, ssDNA has a much shorter persistence length of 0.6nm, similar to commonly used synthetic flexible polymers such as polystyrene (0.9nm). In addition, majority of the synthetic polymers used in industry are flexible polymers, and experimental data on ssDNA will yield increased understanding of the materials that are used and can be further applied in various aspects. The properties of flexible polymer chains are expected to result in enhanced non-linear effects and non-equilibrium dynamics.

Overall, single molecule experiments on ssDNA will yield crucial information on the unique dynamic properties of truly flexible biopolymers, which will enable use of ssDNA in a variety of applications. For example, ssDNA based materials have potential in green chemistry or synthesis of non-natural materials based on green chemistry synthesis routes, with an overall potential to replace many existing synthetic polymers in the market today.

References

[1] R. G. Larson, *The Structure and Rheology of Complex Fluids*., Oxford, New York, (1999).
[2] P. J. Hagerman, *Annu. Rev. Biophys. Biophys. Chem.*, **17,** 265 (1988)
[2] E. S. G. Shaqfeh, *J. Non-Newtonian Fluid Mech*., **130**, 1 (2005).
[3] D. E. Smith, H. P. Babcock, S. Chu, *Science.,* **283**, 1724 (1999).
[4] T. T. Perkins, S. R. Quake, D. E. Smith, S. Chu, *Science*., **264**, 822 (1994).
[5] C. M. Schroeder, H. P. Babcock, E. S. G. Shaqfeh, S. Chu, *Science.,* **301**, 1515 (2003).
[6] C. Haber, D. Wirtz, *Rev. Sci. Instrum.,* **71**, 4561 (2000).
[7] Y. Chan, R. G. Haverkamp, J. M. Hill, *J.Theoretical Biology.,* **262**, 498 (2010).
[8] J. F. Marko, E. D. Siggia, *Macromolecules.,* **28**, 8759 (1995).
[9] N. Ribeck, O. A. Saleh, *Rev. Sci. Instrum.,* **79**, 094301 (2008)
[10] S. B. Smith, Y. J. Cui, C. Bustamante, *Science*, **271**, 795 (1996)
[11] S. B. Smith, L. Finzi, C. Bustamante, *Science.,* **258**, 1122 (1992).
[12] P. Cluzel, A. Lebrun, C. Heller, R. Lavery, J. L. Viovy, D. Chatenay, F. Caron, *Science*, **271**, 792 (1996)
[13] H. Clausen-Schaumann, M. Rief, C. Tolksdorf, H. E. Gaub, *Biophys. J.*, **78**, 1997 (2000)
[14] C. Bustamante, Y. R. Chemla, N. R. Forde, D. Izhaky, *Annual Review of Biochemistry*., **73**, 705 (2004).
[15] J. F. Leger, J. Robert, L. Bourdieu, D. Chatenay, J. F. Marko*, Proc. Natl. Acad. Sci. U.S.A.,* **95**, 12295 (1998)
[16] C. Bustamante, S. B. Smith, J. Liphardt, D. Smith, *Current Opinion in Structural Biology,* **10**, 279 (2000)
[17] T. Morii, R. Mizuno, H. Haruta, T. Okada, *Thin Solid Films.*, **464**, 456 (2004)
[18] J.L. Hutter, J. Bechhoefer, *Review of Scientific Measurements*., **64**, 1868 (1993)
[19] M. L. Bennink, O. D. SchÄrer, R. Kanaar, K. Sakata-Sogawa, J. M. Schins, J. S. Kanger, B. G. de Grooth, J. Greve, *Cytometry.,* **36**, 200 (1999).
[20] R. Nambiar, A. Gajraj, J. Meiners, *Biophysical Journal.,* **87**, 1972 (2004)
[21] M. D. Wang, H. Yin, R. Landick, J. Gelles, S. M. Block, *Biophysical Journal.,* **72**, 1335 (1997)
[22] J. Wang, C. Lu*, J. Applied Physics.,* **102**, 074703 (2007)
[23] C. Goose, V. Croquette, *Biophysical Journal.,* **82**, 3314 (2002)
[24] K. Kim, O. A. Saleh*, Nucleic Acids Research.,* **37**, 20 (2009)
[25] A. J. W. te Velthuis, J. W. J. Kerssemakes, J. Lipfert, N. H. Dekker, *Biophysical Journal.,* **99**, 1292 (2010).
[26] K. Huang, *Statistical Mechanics (2nd ed.).,* 136 (1987)
[27] P. F. Popescu, Wellesly College (2005).
[28] P. A. Wiggins, *Physical Review E.,* **73**, 031906 (2006).
[29] P. C. Hiemenz, T. P. Lodge, *Polymer Chemistry (2nd ed.),* 223 (2007)
[30] F. Zernike, *Physica*., **9**, 686 (1942).

[31] J. C. Crocker, D. G. Grier*, J. Colloid Interface Sci*., **179**, 298 (1996).
[32] E. Toprak, H. Balci, B. H. Blehm, P. R. Selvin, *Nano Letters*., **7**, 2043 (2007)
[33] T. Odijk, *Macromolecules.*, **28**, 7016 (1995).